



Summer 2019

West Virginia Ecological Forecasting
Forecasting red spruce Restoration Using NASA Earth Observations to Support the
USFS Monongahela National Forest

DEVELOP Technical Report
Final Draft – August 9th, 2019

John Dialesandro (Project Lead)
Mason Bull
Tia Francis
Katherine Yut

Keith Weber (Idaho State University, GIS Training and Research Center)
Joseph Spruce (Science Systems and Applications, Inc., Consultant)
Dr. Catherine Jarnevich (United States Geological Survey, Fort Collins Science Center)

1. Abstract

Within the Monongahela National Forest (MNF), situated in the Allegheny Highlands of West Virginia, extensive logging and mining practices have significantly altered the structure and composition of flora and fauna over the past two centuries. Of particular concern to MNF land managers are red spruce (*Picea rubens*) stands, which provide shelter and food to several endangered and threatened species. To aid red spruce restoration, this study mapped current and historical stands and identified non-native stands with suitable habitats for red spruce in the Sharp Knob Red Spruce Restoration Area. Data from Landsat 5 Thematic Mapper (TM), Landsat 8 Operational Land Imager (OLI), and Shuttle Radar Topography Mission (SRTM) were input into classification tree and fuzzy logic algorithms. Furthermore, 2018 classification maps were utilized in the TerrSet Land Change Modeler to forecast red spruce extent up to 2040. As a product of these analyses, we produced three sets of maps: four time series maps of red spruce stands from 1989 to 2018, a map that identifies suitable stands for future restoration efforts, and a red spruce land cover change map up to 2040. Our results indicate that 1,040 hectares are suitable for future restoration in Sharp's Knob, with an 8% gain in red spruce stands from 1989 to 2018. However, forecasting results indicate that management intervention will be necessary for this trend to continue.

Keywords

Landsat 8 OLI, TerrSet, Land Change Modeler, Forest restoration, red spruce

2. Introduction

2.1 Background Information

Forest succession and structure are important ecological factors with wide-ranging implications (Chu & Guo, 2014). Changes in a forest's dominant canopy cover can significantly alter the biophysical characteristics of its ecosystem, including soil morphology, groundwater hydrology, and fauna biodiversity (Nauman et al., 2015; US Forest Service, 2014). Thus, an important goal of sustainable forest management is successful forest regeneration, particularly in ecosystems dominated by non-native species (Vickers et al., 2019). Within these ecosystems, land managers often focus on implementing strategies that reduce non-native species while restoring native species to their historical habitats. However, achieving this result requires meticulous data collection and a thorough understanding of habitat dynamics of the study site. In particular, managers need to know where native species currently thrive and where suitable habitats exist within the management parcel (Falkowski, Evans, Martinuzzi, Gessler, & Hudak, 2009; Nowacki & Wendt, 2010). A thorough understanding of these parameters can facilitate forecasting future species composition and spread under a variety of management, urbanization, and climatic scenarios (Busing, Solomon, McKane, & Burdick, 2007).

This study focuses on the Sharp's Knob Red Spruce Restoration Area – referred to as Sharp's Knob – located in the Monongahela National Forest (MNF). Historically, red spruce (*Picea rubens*) was the dominant canopy cover species. However, extensive logging and mining practices during the early 20th century, in combination with aggressive fire seasons, have significantly altered the landscape (Gundy, Strager, & Rentch, 2012; Lynch & Hessler, 2010; Nowacki & Wendt, 2010). This area of the Monongahela National Forest was heavily mined for over 200 years, but in the 1970s and 1980s, the process of surface mining to extract coal saw a resurgence in southwestern West Virginia (Sams & Beer, 2000). Following this environmental degradation, early restoration efforts focused on planting non-native hardwoods, resulting in a widespread conifer-to-hardwood transition.

This transition from native to non-native tree species has proven problematic given that red spruce not only provides shelter and food for two of MNF's endangered species – the northern flying squirrel (*Glaucomys subrinus fuscus*) and the Cheat Mountain salamander (*Plethodon netting*) – but also facilitates critical soil organic carbon stocks and cultivates absorbent soils near hydrologic headwaters (Nowacki & Wendt, 2010; Nauman & Connolly, 2014; Pauley, 2010; Wooten, Sutton, & Pauley, 2010). The 20th-century conifer-to-hardwood transition resulted in massive losses of soil carbon to the atmosphere (Nauman & Connolly, 2014). However, current literature suggests that restoring historic red spruce stands in West Virginia could reintroduce approximately 6.6 teragrams of carbon to the soil within 80 years (Nauman & Connolly, 2014). Additionally,

the hydraulic holding capacity of red spruce associated soils is a thousand-fold when compared to soils associated with hardwoods, producing important implications for the region's water quality and susceptibility to flooding (Hart, 1959; Mockrin, Lilja, Weidner, Stein, & Carr, 2014).

To aid forest regeneration of red spruce, this study located native species cover, identified suitable native species habitats, and forecasted future extent under specific management scenarios. Previous studies have used high-resolution imagery to detect and classify specific tree species in a mixed forest in addition to detecting tree mortality from drought (Makoto, Tani, & Kamata, 2013). Medium and coarse resolution satellite imagery has been utilized in the same manner, particularly Landsat imagery (Hart et al., 2015) and Sentinel imagery (Soleimannejad, Ullah, Abedi, Dees, & Koch, 2019). Light Detection and Radar (LiDAR) has also been used successfully in unions with multispectral data (Dalponte, Bruzzone, & Gianelle, 2008). For spectral identification and differentiation between species, particularly in distinguishing between coniferous and deciduous stands, imagery stacks have proven effective. Imagery stacks for these analyses often include leaf-on and leaf-off seasons, in addition to vegetation indices such as the Normalized Difference Vegetation Index (NDVI), Infrared Percentage Index (IPVI), Red-Green Ratio Index (RGI), and the Optimized Soil-Adjusted Vegetation Index (OSAVI) (Hart & Veblen, 2015; Xie, Chen, Lu, Li, & Chen, 2019).

2.2 Project Partners

We partnered with the US Forest Service (USFS) Monongahela National Forest and the Northern Institute of Applied Climate Science (NIACS) to explore the feasibility of using NASA Earth observations to guide restoration efforts at Sharp's Knob. Red spruce stands, once restored, can provide the necessary habitats for endangered species, influence soil organic carbon stocks, and improve groundwater hydrology. Our partners will use the maps from this project to guide restoration efforts and management decisions within Sharp's Knob, such as identifying areas to cut nonnative hardwoods and plant red spruce seedlings. Forecasting maps will be similarly used to guide restoration, particularly in justifying the allocation of resources for red spruce restoration as climate variation impacts habitats. Additionally, our partners will replicate our methodology for future red spruce restoration – both to monitor ongoing initiatives and to select future sites.

2.3 Objectives

The objectives for this project were to 1) identify the historical extent of red spruce stands within the study site from 1989 to 2018 using a supervised classification algorithm, 2) conduct a habitat suitability analysis on Sharp's Knob to identify areas suitable for red spruce that are currently dominated by non-native hardwoods, and 3) use the output from objectives 1 and 2 to forecast the extent of red spruce under various management and climate variation scenarios up to 2040. Following the completion of our three main objectives, a well-documented tutorial outlining the workflow of the project was produced. Although the current project focuses on Sharp's Knob, our partners have expressed a strong interest in replicating our methodology for future restoration projects.

2.4 Study Area

The MNF lies in the Alleghany Highlands of eastern West Virginia, with the spine of the southern Appalachians running through its center. MNF encompasses a total area of 6,889 km², making it the largest National Forest in West Virginia. Within its boundaries is Spruce Knob, which is the state's tallest peak at an elevation of 1,481 m. The eastern side of the forest is significantly lower in elevation, lying at 304 m. The majority of the MNF lies within a single Landsat scene, Worldwide Reference System path 17 and row 33. However, the southern corner of the study site lies within path 17, row 34. Per partner request, this project focuses on Sharp's Knob (Figure 1), which entails 52 km² and is at an elevation of approximately 1,381 m.

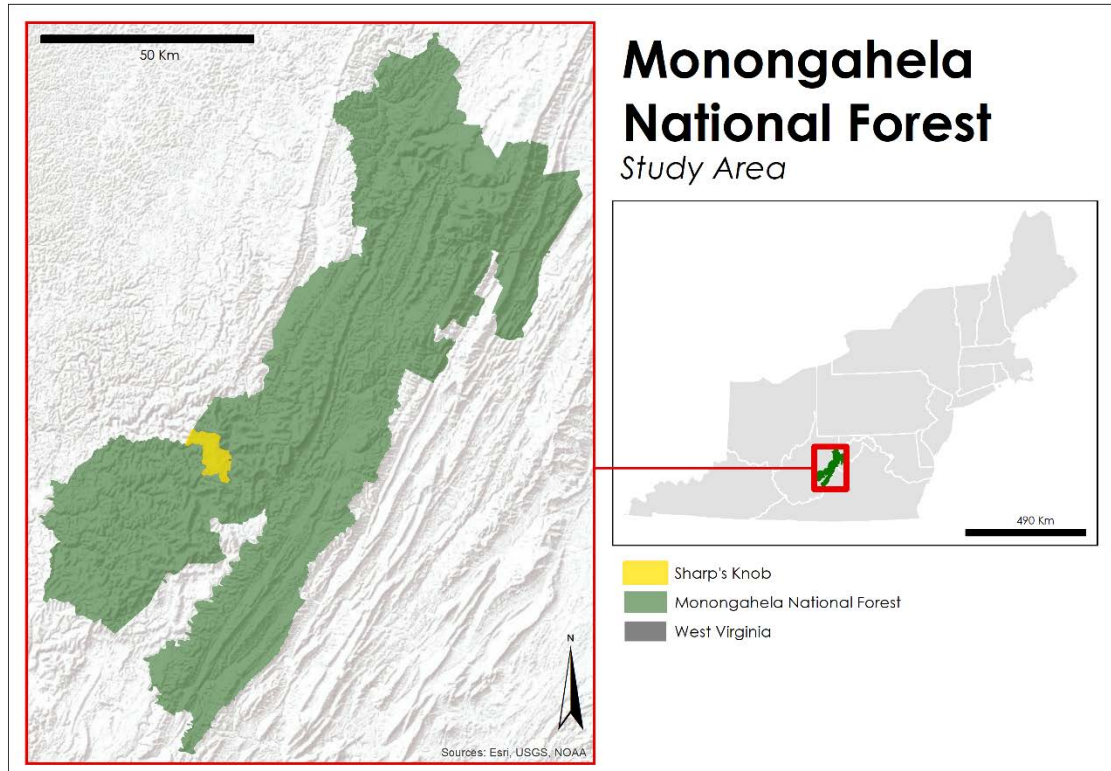


Figure 1. Study area map of Sharp's Knob Red Spruce Restoration Area within the Monongahela National Forest in West Virginia.

3. Methodology

3.1 Data Acquisition

Imagery was ordered and downloaded from the USGS Earth Explorer (EROS) Center Science Processing on-demand interface (USGS, 2016). We downloaded Landsat 8 Operational Land Imager (OLI), and Landsat 5 Thematic Mapper (TM) Surface Reflectance Higher Level data products for path 17, rows 33 and 34 for the summer (leaf-on) and winter (leaf-off) months of 1989, 2001, 2007, and 2018. All leaf on imagery was collected during either July or August, while leaf off imagery was taken from either November or January. These years and months were chosen for analysis due to their high radiometric fidelity across the aforementioned seasons and rows. We also acquired Shuttle Radar Topography Mission (SRTM V2) products downloaded from EROS to provide a 30-meter Digital Elevation Model (DEM) for the study area.

Our partners at the MNF provided us with a shapefile of the administrative boundary of the national forest, as well as the cartographic boundary of the Sharp's Knob restoration site. Unprocessed, high resolution (~10m spatial resolution) orthorectified aerial imagery of West Virginia from 2010 was also provided. Additionally, they provided ground truth point data of red spruce for 2013 and 2013 polygon data of dominant canopy cover derived from orthorectified aerial imagery.

Appendix A, Table A1 outlines the NASA Earth observations and ancillary datasets used for this project.

3.2 Data Processing

Utilizing the TerrSet software from Clark Labs, ENVI 5.5, and Google Earth Engine, we processed and analyzed Landsat 5 TM and Landsat 8 OLI. Processed SRTM DEM, Landsat 5 TM, and Landsat 8 OLI data and imagery, allowed us to derive indices using the Spatial Analyst package in ArcMap and Band Math in

ENVI. As a standard, all geospatial data were projected into WGS 1984 UTM Zone 17N. Processing and analysis consisted of pre-processing for atmospheric correction, mosaicking two scenes, clipping to our study area, generating image derivatives, collecting training data for image classification, and image classification.

3.2.1 Image Derivatives

For both Landsat 5 TM and Landsat 8 OLI, we produced Normalized Difference Vegetation Index (NDVI), Normalized Difference Moisture Index (NDMI), and Built Up Index (BU) and also performed a Principal Components Analysis for each year (Table 1). Although a Normalized Built Index (NDBI) was not included in analysis, it was computed in order to calculate BU. Additionally, aspect and slope were derived from the SRTM DEM (Figure 2).

Table of Image Derivatives Used

Index	Formula	Interpretation
Normalized Difference Vegetation Index	$NDVI = \frac{NIR - Red}{NIR + Red}$ <p>*NIR = near infrared</p>	High positive values near 1 indicate areas with productive and dense vegetation. Low positive values near 0 indicate stressed vegetation or sparse cover. Negative values represent non-vegetated areas, typically water, snow, or bare soil.
Normalized Difference Moisture Index	$NDMI = \frac{NIR - SWIR}{NIR + SWIR}$ <p>*SWIR = shortwave infrared</p>	High positive values near 1 indicate high levels of soil moisture and dense canopy. Low positive values near 0 indicate average canopy cover with high water stress. Negative values indicate bare soil.
Normalized Difference Built Index	$NDBI = \frac{SWIR2 - NIR}{SWIR2 + NIR}$ <p>*SWIR2 = shortwave infrared 2</p>	High positive values near 1 indicate high reflectance areas, such as barren land and urban. Low positive values near 0 indicate vegetation. Negative values indicate bodies of water.
Built-up Index	$BU = NDBI - NDVI$	High positive values near 1 directly indicate urbanized and barren land, with vegetation taken out of the index. Negative values indicate bodies of water.

In

Table 1: Vegetation indices derived from Landsat 5 TM and Landsat 8 OLI

addition to the image derivatives listed above we also derived a principal components analysis (PCA) for each of our 4 years of multispectral imagery. Principal components analysis (PCA) is an orthogonal transformation that minimizes the dimensionality of large data sets based on the statistics of the data (Jolliffe, 2002). PCA

transforms a number of variables in our case multispectral bands to a set of uncorrelated variables called principal components (PCs), all of which contains a linear composite of data variables.

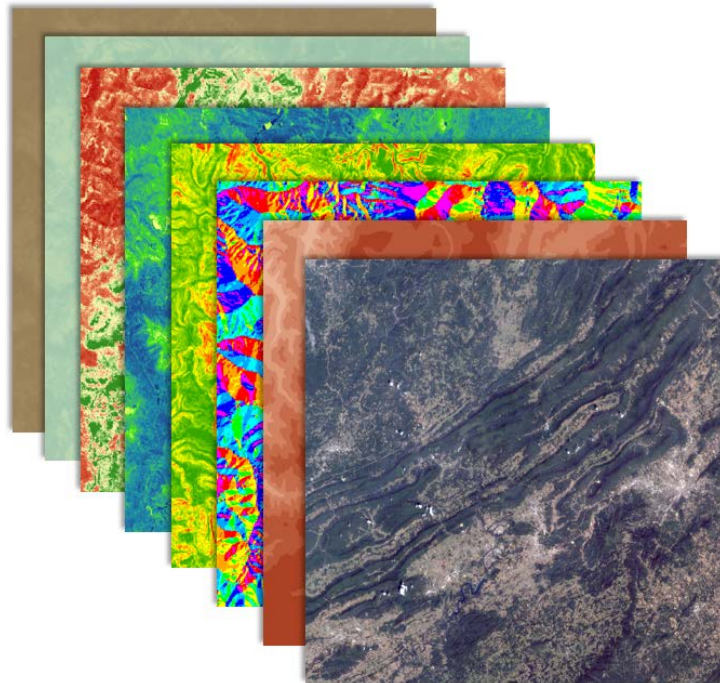


Figure 2: This is a stack of the Landsat and SRTM derivatives used for the Supervised Classification. Landsat derivatives used in this image were from 2018 August imagery. Starting from front to back: Multispectral imagery (blue band to SWIR2), Elevation, Aspect, Slope, NDVI, NDMI, NDBI, and BU.

3.3 Data Analysis

3.3.1 Supervised Classification

To classify the Landsat imagery, we used a Classification Tree Algorithm in TerrSet. The classification was conducted on imagery from the years 1989, 2001, 2007, and 2018. Six classes were identified: urban, deciduous tree, grass, spruce tree, water, and soil. Per our partners, we assumed the conifers present in the study area would be red spruce, so we did not utilize a separate class for non-spruce conifers. Red spruce training points were obtained via *in situ* partner data. Training points for all other classes were collected via digital ocular sampling using NAIP and aerial imagery from our partners for 2007 and 2018 (Figure 3). Digital ocular sampling is placing presence points over high resolution imagery that is interpreted by a person. Since NAIP imagery was largely unavailable for the study area in 2001 and 1989, training data was collected using various false color composites of Landsat 5 TM imagery. At least 120 training points were collected for each class, with a total of approximately 1,500 training points for each classification.



Figure 3: Example of digital ocular sampling using imagery of MNF obtained from our partners. Our six classes were identified by the following numbers: 1 = Spruce Tree, 2 = Deciduous Tree, 3 = Grass, 4 = Soil, 5 = Water, 6 = Urban.

Accuracy of the classifications were determined using a base error matrix output from TerrSet. Base error matrices rely on splitting data points into two separate categories: training and testing. We collected over 1,000 field and image samples for each year. For our classification, 60% of the collected data points were used for training and 40% for testing. The error matrix is then calculated by dividing the number of testing pixels correctly categorized by the overall number of pixels used for testing.

3.3.2 Ecological Forecasting

To further analyze changes between 1989 and 2018 classification outputs and forecast red spruce extent to 2040, classified images were put into TerrSet's Land Change Modeler (LCM). For the purposes of this analysis, a business-as-usual (BAU) model was utilized to forecast red spruce, wherein dynamic variables such as future climatic scenarios or alternative management scenarios were not included. Thus, forecasting results were based on current management strategies and techniques throughout the study period, which include several red spruce restoration projects and initiatives.

LCM allows analysts to comprehensively analyze land cover change by outputting cartographic and graphical figures of change over time using Neural Networks and Markov Chain matrices. MLP is a machine learning algorithm applied to LCM by modeling transition potential due to its ability to capture non-linear relationships (Olmedo, Mas, & Paegelow, 2013). MLP uses a back-propagation algorithm and is based on an input layer, an output layer and hidden layers. Hidden layers lie between input and output layers and work by taking the raw data from input layers and producing the output layer through the appropriate activation function (Frieht, Mulugeta, & Gala, 2015). LCM then uses the transition potentials as inputs into the Markov chain model, where gains, losses, and persistence of classes within the study area between two dates are used to predict future change. This culminates in a transition probability matrix, with values close to 0 representing low probability of transitioning and 1 representing high probabilities (Hamad, Balzter, & Kolo, 2018). A Markov chain model uses gains, losses, and persistence of classes within the study area from one time to another to predict future change. This culminates in a transition probability matrix, with values close to 0 representing low probability and 1 representing high probabilities of transitioning between classes (Hamad, Balzter, & Kolo, 2018). In addition to 1989 and 2018 classification maps, we added data layers representing distance from roads, elevation, aspect, and slope.

3.3.3 Habitat Suitability

Finally, to determine suitable habitats for future restoration projects, we used the Fuzzy membership and overlay algorithms in ArcMap. Relevant variables, their membership types, and midpoint values were determined using a combination of relevant literature and the expert opinion of our partners (Nowacki, Carr, & Dyck, 2010; Nowacki & Wendt, 2010). Thus, the following inputs were utilized: elevation, slope, number of frost days, number of growing degree days, annual mean temperature, annual mean precipitation, and distance from roads, soil pH, soil's percent silt, and soil's percent sand. The climate data were obtained from the Multivariate Adaptive Constructed Analogs (MACA) which is a statistical method for downscaling Global Climate Models at a coarse resolution (Pierce et al. 2014).

Each of the selected variables have demonstrated a statistically significant association with red spruce stands and present limitations to red spruce growth. Not all statistically significant variables were chosen, as it is unclear whether some variables – particularly soil properties such as organic matter or soil carbon stocks – are requisite for a suitable habitat for red spruce or whether red spruce creates a suitable habitat for the culmination of such soil properties. Therefore, such variables should not be included in a habitat suitability model without further investigation into their relationship with red spruce presence.

4. Results & Discussion

4.1 Analysis of Results

4.1.1 Supervised Classification

Our team made four classification maps for the years 1989, 2001, 2007 and 2018 in the Monongahela National Forest and Sharp's Knob restoration area (Figure 4). The classification algorithms for our study area performed best when using bands 2-7 from either Landsat 5 or Landsat 8 for the leaf-on and leaf-off as well as a set of image derivatives. The image derivatives were an NDVI difference image computed using leaf-off imagery, an NDMI image for leaf-on imagery, a BU index image, and the first band of the PCA, elevation, slope, and aspect. Classification performance was quantitatively assessed by using an error matrix generated through the Errmat tool in Terrset. The overall accuracy of our six land cover classifications for our study years were: 83.4% (1989), 84.5% (2001), 78.6% (2007), and 80.8% (2018) (Table 2). In addition, the model's overall Kappa Index of Agreement (KIA) values were 0.783006, 0.804556, 0.729678, 0.755865 respectively. Red Spruce ranged in accuracy from 90.1% user's and 85.1% producer's accuracy in 1989 to 88.9% users and 89.4% producer's accuracy in 2018. Our poorest performing class accuracy was grass, which had as low as 53% accuracy in 2007. This poorer performance could have been due to semi-grassy meadows in recovery stages of mine reclamation being confused with soil. Throughout all four classifications, spruce was most commonly confused with deciduous forest.

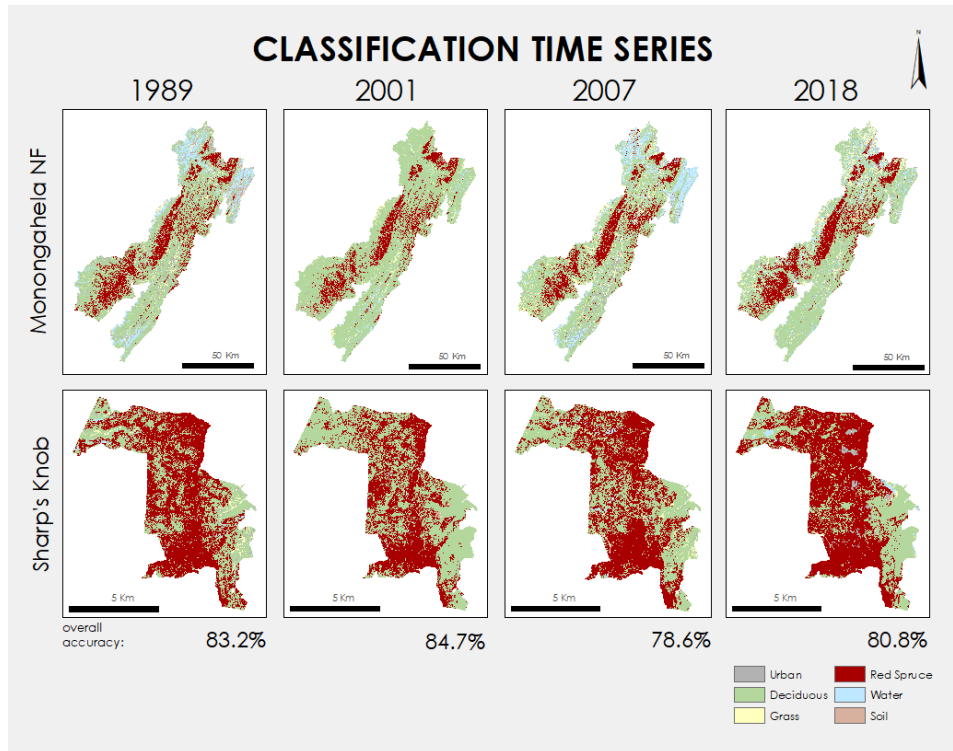


Figure 4: 1989, 2001, 2007, and 2018 classification maps for both the MNF and Sharp's Knob.

Error Matrix of 2018 Land Cover Classification

	Urban	Decid	Grass	Spruce	Water	Soil	Total	Error Commission	User Accuracy
Urban	77	0	6	1	6	6	96	0.198	0.802
Decid	1	57	1	13	2	0	74	0.230	0.770
Grass	7	1	26	1	6	2	43	0.395	0.605
Spruce	3	14	1	152	0	1	171	0.111	0.889
Water	9	3	2	3	48	0	65	0.262	0.738
Soil	7	0	0	0	0	43	50	0.14	0.86
Total	104	75	36	170	62	52	499		
Error Omission	0.260	0.24	0.278	0.106	0.226	0.173		0.192	
Producer Accuracy	0.740	0.76	0.722	0.894	0.774	0.827			

Table 2: Error Matrix of 2018 Land Cover Classifications. Overall Accuracy = 80.85%, Overall Kappa = 0.756.

Land Change Modeler within Terrset was run to determine the change of red spruce extent between 1989 and 2018 and forecast land cover changes to the year 2040. Through the early portion of our study period, red spruce initially declined. However, according to the model, an overall net gain of 17,777 hectares (ha) were reclaimed by red spruce for the entire Monongahela National Forest between 1989 and 2018 (Figure 5). Within

Sharp's Knob our model predicted red spruce reclaimed 238 ha between 1989 and 2018. Spruce regeneration was seen along the edges of Spruce forests, where losses were seen in a less uniform manner throughout the forest clustered in mining regions (See Figure 6). This trend was consistent within Sharp's Knob as well.

Land Cover Changes in Hectares (1989-2018)

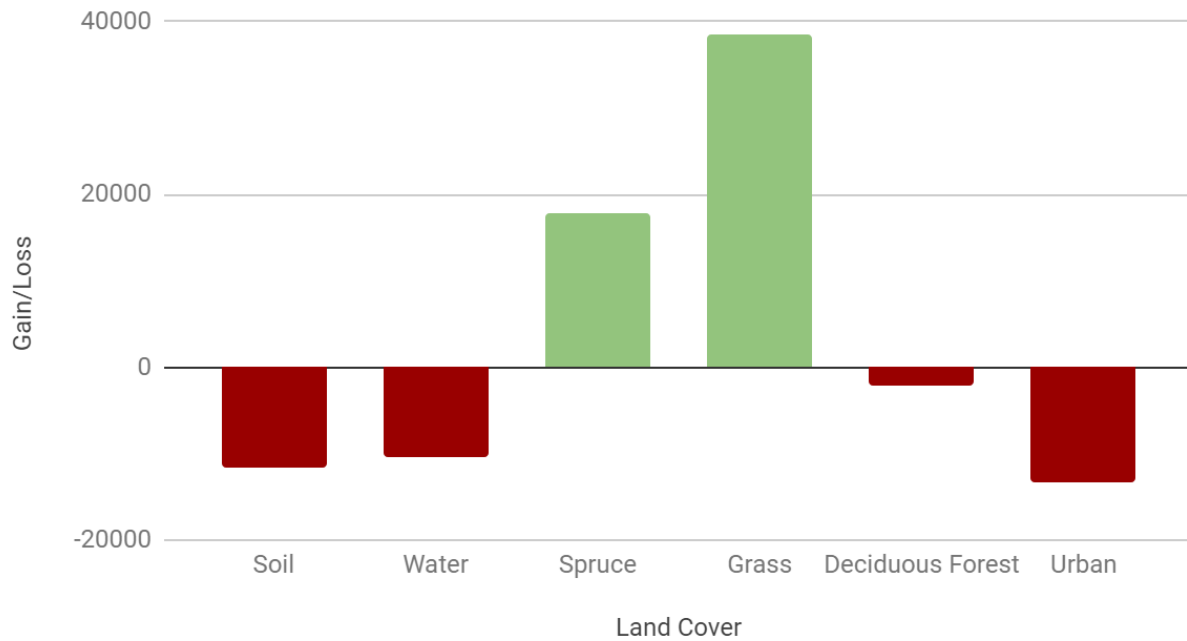


Figure 5: Change in hectares across our classes between 1989 and 2018 with losses in red and gains in green.

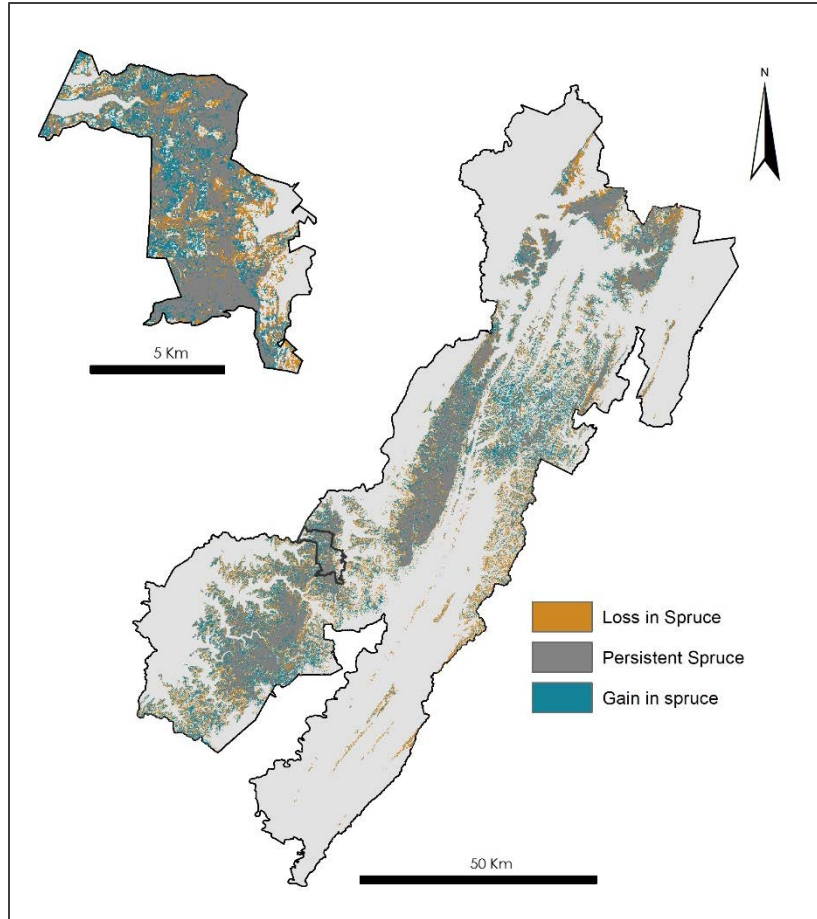


Figure 6: Gains and losses in red spruce in the MNF (left) and Sharp’s Knob (right) between 1989 and 2018.

Additionally, land cover increases in grass and decreases in soil were observed within the model from 1989 to 2018. Overall, soil land cover decreased by 11,634 hectares – of which 45% (5236 ha) were specifically changed to grass. This is important to note as grass is one of the beginning stages of mine reclamation. Deciduous Forest for our study period saw a small decline of 2,039 ha throughout the entire Monongahela National Forest in our 30 year study period. This decline may have been attributed to areas experiencing transition to red spruce through recent restoration efforts.

4.1.2 Ecological Forecasting

Land Change modeler also forecasted changes to 2040 based on the inputs of transition potentials between the 30 previous years of land cover inputted (Table 3). The result based on the model predicted that of the 376,311 ha that were deciduous forest, 11% or 41,394 ha were expected to transition to red spruce based on the past 30 years of changes to red spruce from deciduous. Grass and soil were both predicted that negligible amounts would transition to red spruce habitat even in areas where red spruce was historically present. Additionally, this indicates that management intervention would be necessary for these areas to be optimized.

Probability of Land Cover Change

	Urban	Deciduous Forest	Grass	Spruce	Water	Soil
--	-------	------------------	-------	--------	-------	------

Urban	15.88	51.12	20.71	0	11.36	0.94
Deciduous Forest	2.93	72.06	6.55	10.87	6.17	1.42
Grass	20.93	19.52	52.29	0	6.34	0.92
Spruce	2.03	23.83	0.9	69.86	1.34	2.04
Water	0.15	2.17	0.4	0.04	97.23	0
Soil	21.53	32.89	26.46	3.67	12.48	2.96

Table 3: Transition Probabilities Grid (values in percentage). Row represents “change from,” and columns represent “change to.”

4.1.3 Habitat Suitability

A 30 m resolution Habitat Suitability Map for 2018 was achieved via a fuzzy logic algorithm (Figure 6). Across the entire MNF, 30% (2,381 km²) of the forest was categorized as very high suitability, 19% high suitability (738 km²), 11% (1 km²) medium suitability, and 39% (1,489 km²) low suitability. The low suitability area largely includes roads and low elevation areas of the forest, while the high and very high suitability areas largely includes high elevation areas that are currently dominated by red spruce canopy cover. In Sharp’s Knob, 77% (3,586 ha) of the restoration area was classified as very high suitability, while 14% (654 ha) was classified as high suitability, 2% (139 ha) was classified as medium suitability, and 5% (248 ha) as low suitability. Of the high and very high suitability classifications, approximately 1,040 ha are suitable for restoration according to our model.

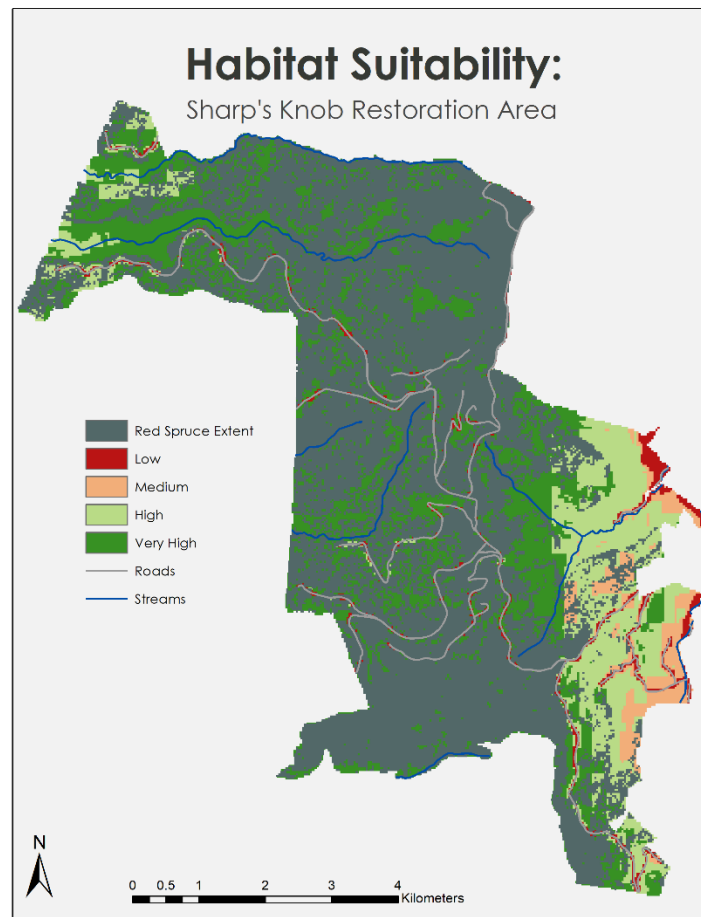


Figure 6: Final habitat suitability map produced for Sharp's Knob. Red spruce extent overlaid on suitability analysis.

Validation of the habitat suitability model suggested high levels of accuracy. Of the 1,284 red spruce validation points used for this study, 79% (1,025 points) fell within the very high classification, while 6% fell within the high classification. Combined, 86% (1,111 points) of the red spruce validation points fell within either a very high or high classification. Additionally, of the points that did not fall within a high or very high classification, 151 points (87%) were located within red spruce core areas, but were close enough to roads to be categorized as within an area of low suitability. Thus, only 22 of these points were outside of red spruce core areas. Additional comparison of high suitability areas against red spruce core areas generated from our classification model further suggest high levels of accuracy. Of all areas classified as red spruce within the forest, 84% were classified in either very high or high suitability areas. According to our model, 982 km² of areas classified as red spruce were in very high suitability areas, while 181 km² were in high suitability areas. Combined, very high and high suitability areas covered 1,162 km² out of a total of 1,386 km² of red spruce.

4.3 Future Work

Classification accuracy could be improved by refining training samples with yearly *in situ* data points. Additionally, image derivatives could be expanded to include soil adjusted vegetation index (SAVI), enhanced vegetation index (EVI), or albedo. Other potential model inputs are roughness, curvature, depth to fragipan, drainage class, available water capacity, organic matter, or bulk density.

A natural extension of this research involves extending our methodology to alternative study sites within the southern Appalachia and historical red spruce extent. Additionally, dynamic variables such as modeled climate variation and alternative management strategies could be added to LCM as variables in our forecasting model. This would allow land managers to explore the effectiveness of proposed restoration initiatives and understand how current red spruce extent and restoration efforts intersect with forecasted climate variation.

5. Conclusions

Historically, red spruce dominated the Monongahela National Forest landscape, but declined during twentieth century mining operations. Initial mining reclamation planted non-native hardwood tree species where red spruce are indigenous. This change in forest composition has threatened endangered species, negatively impacted hydrology, and interfered with carbon sequestering. Recently, recovery efforts have included extensive restoration projects using community engagement and preliminary geospatial analysis.

NASA Earth Observations, such as Landsat 5 TM and Landsat 8 OLI, are well-equipped for remote sensing applications, particularly decision-support for forest restoration. This study demonstrated the applicability of NASA Earth Observations to classify current red spruce extent, forecast future extent, and select suitable habitats. Our models and analyses indicate successful restoration of red spruce extent from 1989 to 2018. However, according to our forecast model, current management strategies are not intensive enough to effectively restore red spruce to its historical extent by 2040. Our Fuzzy Logic habitat suitability analysis suggests that there is still a vast amount of highly suitable acreage for red spruce to reclaim.

The Monongahela National Forest staff will utilize our analysis to prioritize areas of red spruce restoration in the most cost-effective manner. Based on our suitability analysis and the distance between stands, we were able to identify areas of highest opportunity for connectivity. Equipped with these tools and data, the staff can replicate our methodology for future restoration projects outside of Sharp's Knob.

6. Acknowledgments

We would like to thank our partners at the Monongahela National Forest: Stephanie Connolly, Amy Coleman, and Sam Lammie. In addition, we appreciate the advice and expertise of our science advisors, Keith Weber

(Idaho State University, GIS TReC), Joseph Spruce (Science Systems and Applications, Inc.) and Dr. Catherine Jarnevich (USGS Fort Collins Science Center), along with the Colorado & Idaho Center Lead, Kristen Dennis.

Any opinions, findings, and conclusions or recommendations expressed in this material are those of the author(s) and do not necessarily reflect the views of the National Aeronautics and Space Administration.

This material is based upon work supported by NASA through contract NNL16AA05C.

7. Glossary

Conifer – Cone and needle bearing seed plants

Deciduous – Tree or other plant that sheds its leaves in the fall

Earth observations – Satellites and sensors that collect information about the Earth's physical, chemical, and biological systems over space and time

EOS – Earth observing System

Ecological forecasting –Using knowledge of land cover, ecology and other biophysical variables to predict the trajectory of changes in ecosystems, ecological populations, and communities in the future in response to environmental factors like variation in climate

Frost days – An observational day on which frost occurs

Growing degree days – or GDD, a temperature metric that can be used to predict when a crop will reach maturity. Each day's GDD is measured by subtracting a reference temperature, which varies with plant species, from the daily mean temperature.

Hardwood –angiosperm trees that produce lumber and lose their leaves in temperate and boreal forests.

In situ – on site, ground truthed

Landsat-5 TM – Landsat 5 Thematic Mapper (1984-2012)

Landsat-8 OLI – Landsat 8 Operational Land Imager (2013-present)

Normalized Difference Moisture Index (NDMI) – Used to determine water content of vegetation. It uses a ratio between the NIR and SWIR values in traditional fashion

Normalized Difference Vegetation Index (NDVI) – A metric based on the NIR and Red reflectance with high values representing vegetative abundance

Sentinel – European Space Agency multispectral satellite

SOC – Soil Organic Carbon Stock

Support vector machine – supervised learning models with associated learning algorithms that analyze data used for classification and regression analysis.

8. References

Busing, R. T., Solomon, A. M., McKane, R. B., & Burdick, C. A. (2007). Forest dynamics in Oregon

landscapes: Evaluation and application of an individual-based model. *Ecological Applications*, 17(7), 1967-1981. <https://doi.org/10.1890/06-1838.1>

Chu, T., & Guo, X. (2014). Remote sensing techniques in monitoring post-fire effects and patterns of forest recovery in boreal forest regions: a review. *Remote Sensing*, 6, 470-520.

<https://doi.org/10.3390/rs6010470>

Dalponte, M., Bruzzone, L., & Gianelle, D. (2008). Fusion of hyperspectral and LIDAR remote sensing data for classification of complex forest areas. *IEEE Transactions on Geoscience and Remote Sensing*, 46(5), 1416-1427. <https://doi.org/10.1109/TGRS.2008.916480>

Falkowski, M. J., Evans, J. S., Martinuzzi, S., Gessler, P. E., & Hudak, A. T. (2009). Characterizing forest succession with lidar data: An evaluation for the Inland Northwest, USA. *Remote Sensing of Environment*, 113(5), 946-956. <https://doi.org/10.1016/j.rse.2009.01.003>

- Ford, M. W., Moseley, K. R., Stihler, C. W., & Edwards, J. W. (2010). *Area occupancy and detection probabilities of the Virginia Northern Flying Squirrel (Glaucomys sabrinus fuscus) using nest-box surveys* (General Technical Report NRS-P-64). Newtown Square, PA: US Department of Agriculture, Forest Service, Northern Research Station. Retrieved from <https://www.nrs.fs.fed.us/pubs/gtr/gtr-p-64papers/06-ford-p-64.pdf>
- Friehat, T., Mulugeta, G., & Gala, T. S. (2015). Modeling urban sprawls northeastern Illinois. *Journal of Geosciences and Geomatics*, 3(5), 133-141. <https://doi.org/10.12691/jgg-3-5-4>
- Gundy, M. T.-V., Strager, M., & Rentch, T. (2012). Site characteristics of red spruce witness tree locations in the uplands of West Virginia, USA. *Journal of the Torrey Botanical Society*, 139(4), 391-405. <https://dx.doi.org/10.3159/TORREY-D-11-00083.1>
- Hamad, R., Balzter, H., & Kolo, K. (2018). Predicting land use/land cover changes using a CA-Markov Model under two different scenarios. *Sustainability*, 10: 3421-3443. <https://doi.org/10.3390/su10103421>
- Hart, A. C. (1959). *Silvical characteristics of red spruce (Picea rubens)* (Station Paper NE-124). Upper Darby, PA: US Department of Agriculture, Forest Service, Northeastern Forest Experiment Station. Retrieved from <https://www.fs.usda.gov/treesearch/pubs/13710>
- Hart, S. J., & Veblen, T. T. (2015). Detection of spruce beetle-induced tree mortality using high-and medium-resolution remotely sensed imagery. *Remote Sensing of Environment* 168, 134-145. <https://doi.org/10.1016/j.rse.2015.06.015>
- Jolliffe, I. T., (2002). *Principal Component Analysis* (2nd ed.). New York City, NY: Springer. Available from: http://cda.psych.uiuc.edu/statistical_learning_course/Jolliffe%20I.%20Principal%20Component%20Analysis%20%282ed.%20Springer,%202002%29%28518s%29_MVsa_.pdf
- Kautz, S. (2017). Landsat 4-5 Thematic Mapper (TM) Level-1 [Data set]. U.S. Geological Survey. <https://doi.org/10.5066/f7n015tq>
- Kautz, S. (2018). Landsat 8 OLI (Operational Land Imager) and TIRS (Thermal Infrared Sensor) [Data set]. U.S. Geological Survey. <https://doi.org/10.5066/f71835s6>
- Lynch, C., & Hessler, A. (2010). Climatic controls on historical wildfires in West Virginia, 1939-2008. *Physical Geography*, 31(3), 254-269. <https://doi.org/10.2747/0272-3646.31.3.254>
- Makoto, K., Tani, H., & Kamata, N. (2013). High-resolution multispectral satellite image and a postfire ground survey reveal prefire beetle damage on snags in Southern Alaska. *Scandinavian Journal of Forest Research*, 28(6), 581-585. <https://doi.org/10.1080/02827581.2013.793387>
- Mockrin, M. H., Lilja, R. L., Weidner, E., Stein, S. M., & Carr, M.A. (2014). *Private forests, housing growth, and America's water supply: A report from the Forests on the Edge and Forests to Faucets Projects* (General Technical Report RMRS-GTR-327). Fort Collins, CO: US Department of Agriculture, Forest Service, Rocky Mountain Research Station. Retrieved from <https://www.fs.usda.gov/treesearch/pubs/47201>
- Nauman, T. W., Thompson, J. A., Teets, S. J., Dilliplane, T. A., Bell, J. W., Connolly, S. J., ... Yoast, K. M. (2015). Ghosts of the forest: Mapping pedomemory to guide forest restoration. *Geoderma*, 247-248, 51-64. <https://doi.org/10.1016/j.geoderma.2015.02.002>
- Nowacki, G., Carr, R., & Dyck, M. V. (2010). *The current status of red spruce in the Eastern United States: Distribution, population trends, and environmental drivers* (General Technical Report NRS-P-64). Newtown Square, PA:

- US Department of Agriculture, Forest Service, Northern Research Station. Retrieved from: <https://www.nrs.fs.fed.us/pubs/gtr/gtr-p-64papers/35-pauley-p-64.pdf>
- Nowacki, G., & Wendt, D. (2010). *Overview of the status of the Cheat Mountain Salamander* (General Technical Report NRS-P-64). Newtown Square, PA: US Department of Agriculture, Forest Service, Northern Research Station. Retrieved from <https://www.fs.usda.gov/treesearch/pubs/36071>
- Olmedo, C. M. T., Paegelow, M., Mas, J. F. (2013) Interest in intermediate soft-classified maps in land change model validation: suitability versus transition potential. *International Journal of Geographical Information Science*, 27(12): 2343–2361. <http://dx.doi.org/10.1080/13658816.2013.831867>
- Pauley, T. K. (2010). *Characterization of the ecological requirements for three plethodontid salamander species* (General Technical Report NRS-P-64). Newtown Square, PA: US Department of Agriculture, Forest Service, Northern Research Station. Retrieved from <https://www.nrs.fs.fed.us/pubs/gtr/gtr-p-64papers/47-wooten-p-64.pdf>
- Pierce, D. W., Cayan, D. R., & Thrasher, B. L. (2014). Statistical downscaling using localized constructed analogs (LOCA). *Journal of Hydrometeorology*, 15(6), 2558-2585. <https://doi.org/10.1175/JHM-D-14-0082.1>
- Sams, J. I., & Beer, K. M. (2000). *Effects of coal-mine drainage on stream water quality in the Allegheny and Monongahela River basins—Sulfate transport and trends* (Water Resources Investigations Report, 99-4208). Reston, VA: US Geological Survey. <https://doi.org/10.3133/wri994208>
- Soleimannejad, L., Ullah, S., Abedi, R., Dees, M., & Koch, B. (2019). Evaluating the potential of Sentinel-2, Landsat-8, and IRS satellite images in tree species classification of Hyrcanian forest of Iran using random forest. *Journal of Sustainable Forestry*, 38(6). <https://doi.org/10.1080/10549811.2019.1598443>
- Nauman, T. W., & Connolly, S. J. (2014). Red spruce (*Picea rubens*) influence on soil organic carbon (SOC) stocks. Elkins, WV: Monongahela National Forest. Retrieved from: http://restoreredspruce.org/wp/wp-content/uploads/2014/06/white_paper_spruce_soil_carbon_fs_wvu_general_2014.pdf
- Vickers, L. A., McWilliams, W. H., Knapp, B. O., D'Amato, A. W., Saunders, M. R., Shifley, S. R., ... Westfall, J. A. (2019). Using a tree seedling mortality budget as an indicator of landscape-scale forest regeneration security. *Ecological Indicators*, 96, 718-727. <https://doi.org/10.1016/j.ecolind.2018.06.028>
- Wooten, J. A., Sutton, W. B., & Pauley, T. K. (2010). *The current distribution, predictive modeling, and restoration potential of red spruce in West Virginia* (General Technical Report NRS-P-64). Newtown Square, PA: US Department of Agriculture, Forest Service, Northern Research Station. Retrieved from <https://www.fs.usda.gov/treesearch/pubs/36071>
- Wulder, M. A., White, J. C., Loveland, T. R., Woodcock, C. E., Belward, A. S., Cohen, W. B., & Roy, D. P. (2016). The global Landsat archive: Status, consolidation, and direction. *Remote Sensing of Environment*, 185, 271-283. <https://doi.org/10.1016/j.rse.2015.11.032>
- Xie, Z., Chen, Y., Lu, D., Li, G., & Chen, E. (2019). Classification of land cover, forest, and tree species classes with ZiYuan-3 multispectral and stereo data. *Remote Sensing*, 11(2), 164. <https://doi.org/10.3390/rs11020164>

9. Appendices

Table A1
Earth Observations and Ancillary Data

Platform & Sensor	Parameters	Use
Landsat 5 TM	surface reflectance, NDVI, NDMI, NDBI, and BU	Landsat 5 TM data were used to analyze land cover (1989, 2001, 2007), and land cover change and create image derivatives such as NDVI and NDMI for forecast inputs.
Landsat 8 OLI	surface reflectance, NDVI, NDMI, NDBI, and BU	Landsat 8 OLI data were used to analyze land cover (2018), and land cover change and create image derivatives such as NDVI and NDMI for forecast inputs
SRTM	elevation, slope, aspect	This dataset was used to determine topographic derivatives that are correlated with the classification of red spruce and habitat suitability analysis.
Ancillary Data	Parameters	Use
NAIP	high-resolution imagery (1 meter)	This dataset provided high-resolution imagery for the collection of training and testing points via digital ocular sampling.
MACA	Multivariate Adaptive Constructed Analogs Global Climate Model Datasets (Growing Degree Days, Frost free days, Annual Mean Temperature, Annual Mean Precipitation) 1971-2000	These datasets provided regional climatic variables for the habitat suitability analysis at a 4km resolution. Climatic variables were derived using the MACA statistical method, wherein globally fitted climate models are downscaled for national and regional use.
USDA Land Cover Data	USFS Monongahela National Forest <i>in situ</i> datasets	These datasets include point data for red spruce, in addition to polygon coverage of other species to be used in the classification algorithm.
ISRIC Soil Data	Soil pH, soil's % silt, soil's % sand	These datasets provided 250m resolution of predicted soil properties and classifications based on fitted models. Data were utilized as inputs into the habitat suitability model.

Table A2 2007 Error Matrix

	Urban	Decid	Grass	Spruce	Water	Soil	Total	Error Commission	User Accuracy
Urban	70	0	4	0	3	13	90	0.222222	0.777778
Decid	5	64	0	17	1	0	87	0.264368	0.735632
Grass	12	0	28	4	4	4	52	0.461538	0.538462
Spruce	2	10	1	146	1	1	161	0.093168	0.906832
Water	7	1	3	2	53	3	69	0.231884	0.768116
Soil	8	0	0	1	0	31	40	0.225	0.775
Total	104	75	36	170	62	52	499		1
Error Omission	0.326923	0.146667	0.222222	0.141176	0.145161	0.403846		0.214429	0.785571
Producer Accuracy	0.673077	0.853333	0.777778	0.858824	0.854839	0.596154			

Table A3 2001 Error Matrix

	Urban	Decid	Grass	Spruce	Water	Soil	Total	Error Commission	User Accuracy
Urban	56	0	2	0	0	6	64	0.125	0.875
Decid	0	71	1	27	1	0	100	0.29	0.71
Grass	5	0	30	0	0	3	38	0.210526	0.789474
Spruce	0	11	0	145	1	0	157	0.076433	0.923567
Water	1	0	0	1	49	0	51	0.039216	0.960784
Soil	4	0	6	2	0	42	54	0.222222	0.777778
Total	66	82	39	175	51	51	464		
Error Omission	0.1515	0.1341	0.2307	0.17142	0.03921	0.17647		0.153017	
Producer Accuracy	0.8484	0.8658	0.7692	0.82857	0.96078	0.82352	1	0.846983	0.848485

Table A4 1989 Error Matrix

	Urban	Decid	Grass	Spruce	Water	Soil	Total	Error Commission	User Accuracy
Urban	61	7	10	0	0	0	78	0.217949	0.782051
Decid	1	72	0	31	0	3	107	0.327103	0.672897
Grass	6	0	45	0	0	0	51	0.117647	0.882353
Spruce	0	14	0	184	0	6	204	0.098039	0.901961
Water	0	1	4	1	49	1	56	0.125	0.875
Soil	5	0	2	0	0	46	53	0.132075	0.867925
Total	73	94	61	216	49	56	549		
Error Omission	0.1643	0.2340	0.2622	0.14814	0	0.17857		0.167577	
Producer Accuracy	0.8356	0.7659	0.7377	0.85185	1	0.821429			0.832423